THE ASTROPHYSICAL JOURNAL, 583:L67–L70, 2003 February 1

GAMMA-RAY BURST HUBBLE DIAGRAM TO $z = 4.5$

BRADLEY E. SCHAEFER
Department of Astronomy, University of Texas at Austin, RLM 17.226, C-1400, Austin, TX 78712
Received 2002 July 30; accepted 2002 December 18; published 2003 January 10

ABSTRACT

Gamma-ray bursts (GRBs) are tremendous explosions visible across most of the universe, certainly out to redshifts of $z = 4.5$ and likely out to $z \sim 10$. Recently, GRBs have been found to have a roughly constant explosive energy as well as to have two luminosity indicators (the spectral lag time and the variability) that can be used to derive the burst's luminosity distance from the gamma-ray light curve alone. There currently exists enough information to calibrate luminosity distances and independent redshifts for nine bursts. From these, a GRB Hubble diagram can be constructed, in which the observed shape of the curve provides a record of the expansion history of our universe. The current nine-burst diagram is sparse, yet formal limits can be placed on the mass density of a flat universe. This first GRB Hubble diagram provides a proof of concept for a new technique in cosmology at very high redshifts. With the launch of the *Swift* satellite in 2003, we should get ~120 bursts to produce a Hubble diagram impervious to all effects of dust extinction and out to redshifts impossible to reach by any other method.

Subject headings: cosmological parameters — cosmology: observations — distance scale — gamma rays: bursts

1. INTRODUCTION

As always in astronomy, the determination of distances is a crucial and difficult problem. Until recently, the distance scale of gamma-ray bursts (GRBs) was unknown by over 12 orders of magnitude. In 1997, the discovery of optical and radio counterparts (Costa et al. 1997; van Paradijs et al. 1997; Frail et al. 1997) proved that at least the long-duration bursters were at cosmological distances with redshifts of $z \sim 1$. The measurement of GRB redshifts requires deep optical spectra, and to date, only 24 redshifts are known for bursts with unknown selection effects.

If GRB distance indicators can be found that use only gamma-ray data, then we can measure the demographics and cosmology of large and well-understood samples of bursts. Two such luminosity (and hence distance) indicators recently have been proposed. The first (Norris, Marani, & Bonnell 2000) relates the burst luminosity (L) with the spectral lag ($\tau_{\rm lag}$), which can be idealized as the time between peaks as recorded at high and low photon energies. The second (Fenimore & Ramirez-Ruiz 2000) relates the luminosity with the variability (V), which is a specific measure of the "spikiness" of the burst light curve. High-luminosity bursts have short lags and spiky light curves, while low-luminosity events have long lags and smooth light curves. These two relations make GRBs into "standard candles," in the same sense as for Cepheids and supernovae in which an observed light-curve property can yield the luminosity and then the distance.

The two luminosity indicators were originally proposed and calibrated with six or seven bursts. The addition of three or two further bursts (for a total of nine) has fallen on the original relations, hence adding confidence in their utility. Further, if both the $L/\tau_{\rm lag}$ and the L/V relations are true, then there must be a particular $\tau_{\rm lag}/V$ relation, and this prediction has been strongly confirmed with an independent sample of 112 BATSE bursts (Schaefer, Deng, & Band 2001). Finally, the very long lag bursts have been shown to be very low luminosity, as demonstrated by their concentration to the local supergalactic plane (Norris 2002).

These luminosity indicators have been used to identify specific bursts (Fenimore & Ramirez-Ruiz 2000) that are at redshifts of $z \sim 10$ as well as to show that the star formation rate of the universe is rising steadily (Fenimore & Ramirez-Ruiz 2000; Schaefer et al. 2001; Lloyd-Ronning, Fryer, & Ramirez-Ruiz 2002) from $z \sim 2$ to $z > 6$. This Letter reports on the construction of a Hubble diagram (a plot of luminosity distance, D_L, vs. redshift) as a means of measuring the expansion history of our universe.

2. GRB HUBBLE DIAGRAM

Only nine GRBs have the required information of redshift (z), peak flux (P), lag time ($\tau_{\rm lag}$), and variability (V). These data are collected in Table 1, along with the characteristic photon energy ($E_{\rm peak}$) and the observed luminosity ($L_{\rm obs}$). These nine bursts were all detected by BATSE with redshifts measured from optical spectra of either the afterglow or the host galaxy. The highly unusual GRB 980425 (associated with supernova SN 1998bw) is not included, because it is likely to be qualitatively different from the classical GRBs. Bursts with redshifts that were not recorded by BATSE cannot (yet) have their observed parameters converted to energies and fluxes that are comparable with BATSE data.

Simplistically, plots of $L_{\rm obs}$ versus $\tau_{\rm lag}$ and $L_{\rm obs}$ versus V can calibrate the luminosity indicators, which then can yield luminosity distances to each burst for plotting on a Hubble diagram and fitting to cosmological models. In practice, there must be a simultaneous χ^2 minimization for the luminosity calibrations and the cosmology, so as to avoid the effects of possible correlations between the indicators and distance.

If the Earth is not along the central axis of the GRB's jet, then various off-axis effects will change the observed properties. For light viewed off-axis by angle θ from a jet moving at β times the speed of light, the transverse Doppler shift, redshift, and beaming will change the various observed properties by powers of $B = (1 - \beta)/(1 - \beta \cos\theta)$. The observed value of $E_{\rm peak}$ will scale as B, $\tau_{\rm lag}$ will scale as B^{-1}, V will scale as the inverse of a time and hence as B, while L will have a model-dependent variation that scales roughly as B^3. For structured jets (Rossi, Lazzati, & Rees 2002; Zhang & Mészáros 2002), the luminosity and bulk Lorentz factor can be parameterized as being proportional to some positive power of B. When viewed on-axis, the bursts will presumably display fairly

TABLE 1

GRB Luminosity Distances from Lags and Variabilities

GRB	z	P[a] (photons s^{-1} cm^{-2})	τ_{lag}[b] (s)	V[c]	E_{peak}[d] (keV)	log L_{obs}[e] (ergs s^{-1})	log L_{comb}[f] (ergs s^{-1})	D_L[g] (Mpc)
970508	0.84	1.2 ± 0.1	0.307 ± 0.065	0.0010 ± 0.0010	137 ± 14	50.89 ± 0.04	50.70 ± 0.39	4600 ± 2100
970828	0.96	4.9 ± 0.1	0.028 ± 0.007	0.0078 ± 0.0006	176 ± 4	51.65 ± 0.01	51.97 ± 0.26	9600 ± 2900
971214	3.41	2.3 ± 0.11	0.010 ± 0.004	0.0175 ± 0.0012	107 ± 6	52.69 ± 0.02	52.62 ± 0.27	29500 ± 9100
980703	0.97	2.6 ± 0.12	0.147 ± 0.056	0.0025 ± 0.0005	181 ± 9	51.38 ± 0.02	51.16 ± 0.28	5200 ± 1700
990123	1.60	16.6 ± 0.24	0.015 ± 0.005	0.0120 ± 0.0005	267 ± 3	52.74 ± 0.01	52.49 ± 0.26	9500 ± 2900
990506	1.30	22.2 ± 0.27	0.011 ± 0.004	0.0320 ± 0.0080	280 ± 30	52.64 ± 0.01	52.94 ± 0.29	13800 ± 4600
990510	1.62	10.2 ± 0.2	0.012 ± 0.003	0.0352 ± 0.0014	74 ± 2	52.54 ± 0.01	52.65 ± 0.26	14600 ± 4400
991216	1.02	82.1 ± 0.5	0.0050 ± 0.0020	0.0152 ± 0.0003	250 ± 3	52.95 ± 0.01	52.68 ± 0.27	5400 ± 1600
000131	4.5	1.8 ± 0.2	0.0009 ± 0.0004	0.0121 ± 0.0018	183 ± 15	52.86 ± 0.05	53.08 ± 0.28	57000 ± 18500

[a] Peak flux for the brightest 256 ms time interval for 50–300 keV (Paciesas et al. 1999).

[b] Lag as calculated from the peak of the cross-correlation between BATSE channels 3 and 1 using data brighter than 10% of the peak flux (Norris et al. 2000; Norris 2002). These lags have been corrected by $1 + z$ to the frame of the GRB. The quoted 1 σ measurement uncertainties in the log of the lag should be added in quadrature with 0.35, the population dispersion, to get the effective uncertainty for luminosity determination.

[c] Variability following the definition of Fenimore & Ramirez-Ruiz (2000), where V is the normalized variance of the light curve around a $0.15T_{90}$ box-smoothed light curve. The quoted 1 σ measurement uncertainties in the log of the variability should be added in quadrature with 0.20, the population dispersion, to get the effective uncertainty for luminosity determination.

[d] Photon energy of the peak in the νF_ν spectrum, as measured by Mallozzi et al. (1995) with BATSE data.

[e] The base-10 logarithm of the observed luminosity, calculated as $4\pi P\epsilon D_L^2$, where $\epsilon \approx 1.7 \times 10^{-7}$ ergs as the average energy of a photon in the 50–300 keV range and D_L is the luminosity distance that is taken from z for an assumed flat universe with $\Omega_m = 0.3$ (with eqs. [14], [15], [16], and [21] of Hogg 1999). The calculated observed luminosity depends on the adopted Hubble constant (here taken as 65 km s^{-1} Mpc^{-1}), although the cosmology depends only on the *shape* of the Hubble diagram and hence is independent of the Hubble constant.

[f] The base-10 logarithm for the combined luminosity, calculated as the weighted average of the results of eqs. (1) and (2) (for which $\Omega_m = 0.3$ has been adopted).

[g] The luminosity distance calculated as $(L_{comb}/4\pi P\epsilon)^{0.5}$, for luminosity based on an $\Omega_m = 0.3$ calibration.

tight lag/luminosity and variability/luminosity relations. These relations can be converted to similar relations involving observed off-axis quantities with an extra factor of B to some power. Fortunately, the observed distribution of E_{peak} is remarkably narrow for bursts of a given brightness (Mallozzi et al. 1995; Brainard et al. 1999), and the removal of kinematic effects shows that the on-axis E_{peak} is virtually constant (Schaefer 2003). Thus, E_{peak} should be proportional only to some power of B, and this relation can be used to convert the B dependency of the luminosity relations into an E_{peak} dependency. Essentially, we can use the observed E_{peak}-value to get information about the off-axis angle and correct the observed τ_{lag}- and V-values to those that would be seen on-axis. In practice, the correction factor can be taken as some power of $E_{peak}(1 + z)/400$ keV. (The division by 400 keV is to minimize correlations between the normalization constant and the exponent during the fits.) The exponents of the correction factors will be free parameters that depend on the scenario and jet structure.

With the off-axis correction, the luminosities can be derived by fitting the relations $L \propto \tau_{lag,\,corr}^{\alpha_{lag}}$ and $L \propto V_{corr}^{\alpha_V}$, where $\tau_{lag,\,corr} = \tau_{lag}[E_{peak}(1 + z)/400]^{e_{lag}}$ and $V_{corr} = V[E_{peak}(1 + z)/400]^{e_V}$. Plots of L_{obs} versus $\tau_{lag,\,corr}$ and L_{obs} versus V_{corr} for the nine bursts with known redshifts (see Fig. 1) have slopes of α_{lag} and α_V, while the scatter in these plots will be minimized for the best values of e_{lag} and e_V. This gives $\alpha_{lag} = -1.27 \pm 0.20$, $\alpha_V = 1.57 \pm 0.17$, $e_{lag} = 0.6 \pm 0.7$, and $e_V = 0.85 \pm 0.40$. Thus,

$$L = 10^{50.03}\{\tau_{lag}[E_{peak}(1 + z)/400]^{0.6}\}^{-1.27}, \quad (1)$$

$$L = 10^{55.32}\{V[E_{peak}(1 + z)/400]^{0.85}\}^{1.57}, \quad (2)$$

where L is in ergs s^{-1}, τ_{lag} is in seconds, V is dimensionless,

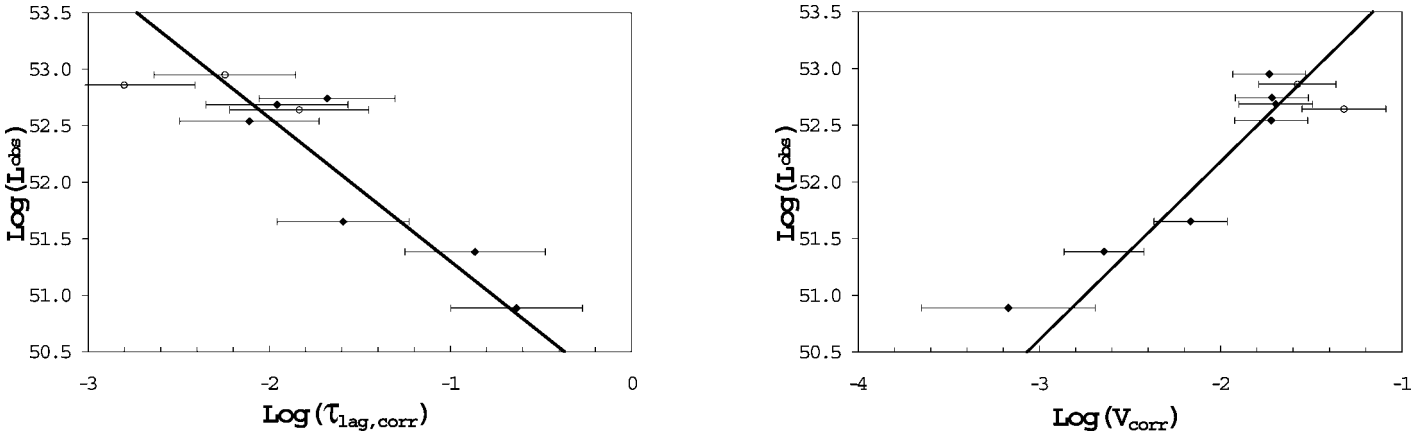

FIG. 1.—Calibration curves for lag and variability. Plots of the observed luminosity vs. lag and variability can be used to calibrate the luminosity indicators. Sufficient data are available for only nine bursts with redshifts. The plots here can be fitted to produce eqs. (1) and (2) (displayed as the straight lines in the two panels). The displayed error bars include not only the observed measurement uncertainties but also the intrinsic scatter for the burst population of 0.35 and 0.20 (for lag and variability, respectively) in logarithmic units, as determined by making the reduced χ^2 of the fits close to unity.

and $E_{\rm peak}$ is in keV. As independent checks, a plot of $\tau_{\rm lag,\,corr}$ versus $V_{\rm corr}$ for 93 BATSE bursts will have a slope of $\alpha_{\rm lag}/\alpha_V$, and the scatter will be minimized for the best values of $e_{\rm lag}$ and e_V. This gives $\alpha_{\rm lag}/\alpha_V = -0.7 \pm 0.2$, $e_{\rm lag} = 0.0 \pm 0.3$, and $e_V = 1.1 \pm 0.3$, values that are consistent with the calibration from Figure 1.

The lag and the variability produce two independent luminosity values through equations (1) and (2). These can be combined as weighted averages (with the weights equal to the inverse square of the 1 σ errors) to produce a combined luminosity ($L_{\rm comb}$) and then D_L, as given in Table 1. A plot of D_L versus z is a Hubble diagram (Fig. 2).

Equations (1) and (2) are optimal for studies of GRBs in which the cosmology is not in question. When the goal is to use the bursts as cosmological markers, care must be taken to avoid circular logic. In particular, the previous paragraph assumed a specific cosmology ($\Omega_m = 0.3$ for a flat universe and $H_0 = 65$ km s^{-1} Mpc^{-1}) for calculating the D_L-values as a function of z. To avoid this circularity, the fits must be performed with the cosmological parameters as additional fit parameters. That is, the model being fitted to the data will have cosmological plus GRB parameters that are to be simultaneously determined by the minimization of the χ^2. This will tie the cosmology conclusions into GRB calibrations, but both will be well constrained when many bursts are available. A correct procedure to find the best value of Ω_m in a flat universe is to (1) fix Ω_m, (2) derive D_L and $L_{\rm obs}$ for each burst for that cosmology, (3) fit $L_{\rm obs}$ as power laws of $\tau_{\rm lag,\,corr}$ and $V_{\rm corr}$, (4) use the best fits to derive $L_{\rm comb}$ and then D_L for each burst, (5) calculate χ^2 by comparing the model and observed D_L-values, (6) repeat steps 1–5 to identify the best-fit Ω_m-value as that in which χ^2 is minimized, and (7) identify the 1 σ range in which χ^2 is within unity of its minimum value. By this procedure, the lowest χ^2 corresponds to $\Omega_m = 0.05$ with the 1 σ constraint $\Omega_m < 0.35$. The 3 σ limit is larger than unity, so this particular measure is not helpful for cosmology. This new result is completely independent of, yet in agreement with, those from supernovae and other methods (Durrer & Novosyadlyj 2001). However, the current value for Ω_m is not yet of high reliability, because the number of degrees of freedom in the fit are small and the slope of the Hubble diagram is dominated by just two high-redshift events. While this new result does not seriously constrain current cosmology, it does act as a demonstration of principle and a sign for the future.

3. COMPARISON WITH SUPERNOVAE

A comparison with the supernova-based Hubble diagram is inevitable. GRBs have both advantages and disadvantages when compared to supernovae. At least currently, supernovae have an advantage over GRBs for the accuracy of the distance measurements for a single event. Well-observed nearby Type Ia supernovae have an rms scatter about their Hubble diagram of 0.18 mag (Phillips et al. 1999), which translates into an uncertainty in the log of the distance of 0.04. GRBs currently have an rms scatter about their calibration curves of 0.35 and 0.20 in the logs of lag and variability, which translates into uncertainties in the log of the distance of 0.22 and 0.16, respectively. These two independent measures can be combined to give an uncertainty of 0.13 in the log of the distance. Thus, individual supernovae are roughly 3 times more accurate as standard candles than are individual GRBs.

The physics of gamma-ray emission from relativistic shocks in GRBs is largely known (but how to create the magnetic fields is not), although the explosion scenario is still uncertain. The basic physics of supernovae is well known (although the Type Ia progenitors still are not identified). Supernovae can have their decline rate versus luminosity calibration from low-redshift events, and this allows the elegance of being able to make the calibration substantially separate from the cosmology. Thus, supernovae are much better understood than are GRBs, and this will be a substantial comfort for using them as standard candles. Nevertheless, it is unclear where this advantage for supernovae will pay off. Currently, the analyses of both supernova and GRB Hubble diagrams are entirely empirical with no contribution from theory, so a better theoretical understanding of supernovae has not helped in any specific manner. Supernovae will have better known evolution effects; yet Branch et al. (2001) show that evolution is no problem for supernovae, and their argument applies identically to GRBs.

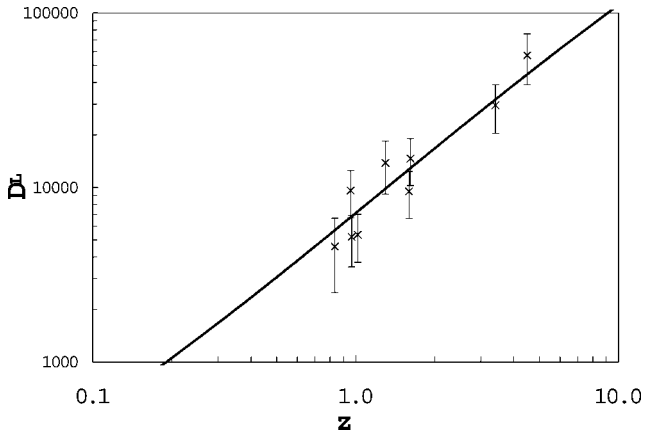

FIG. 2.—GRB Hubble diagram. This Hubble diagram is for nine bursts from $0.84 < z < 4.5$. With *Swift*, we should soon have ~120 bursts from roughly $0.1 < z < 10$, and this will allow a precision measure of the expansion history of the universe to unprecedented high redshifts. The particular diagram above was made for luminosity indicators calibrated assuming a flat $\Omega_m = 0.3$ universe (as in Fig. 1 and eqs. [1] and [2]), and the χ^2 for the data vs. the cosmological model (the curve in the figure) is 6.2. The best-fit cosmology can be found by minimizing the resulting χ^2, as the cosmological model varies both the calibration curves and the resulting Hubble diagram.

Supernovae have substantial problems with a higher dust density at high redshift (Totani & Kobayashi 1999) and the possibility of gray dust (Aguirre 1999). Gamma radiation suffers from no extinction. After a tremendous observational effort, the current supernova Hubble diagram (Perlmutter et al. 1999) extends only out to $z = 0.97$. (SN 1997ff at $z \sim 1.7$ has very large uncertainties [Riess et al. 2001], even without the large corrections for gravitational lensing [Lewis & Ibata 2001; Moertsell, Gunnarsson, & Goobar 2001] and the uncertainty of the supernova type.) The dedicated *Supernova/Acceleration Probe* (*SNAP*) satellite,[1] proposed for launch in 2008, will go out to $z = 1.7$ with exquisite accuracy in the light curves. In contrast, the GRB Hubble diagram is already out to $z = 4.5$, and it likely will be extended to $z \sim 10$ (Fenimore & Ramirez-Ruiz 2000; Lloyd-Ronning et al. 2002) or farther (Lamb & Reichart 2000; Bromm & Loeb 2002). With the launch of the *Swift* satellite in 2003, the GRB Hubble diagram will be available for the redshift ranges $1 < z < 1.7$ and $1.7 < z \lesssim 10$ roughly 5 years before *SNAP* can extend the supernova Hubble diagram only to $1 < z < 1.7$.

In summary, GRBs are ~3 times worse in accuracy than

[1] *SNAP* Collaboration 2002, http://snap.lbl.gov.

supernovae, but this is traded off for the lack of problems from extinction, extension to $z \sim 10$, and an answer many years before *SNAP*. I do not think that the GRB Hubble diagram will replace the supernova Hubble diagram. The reason is that *both* diagrams will have known and unknown systematic problems that will make results from any *one* method not conclusive. What is needed is the concurrence of multiple independent methods. Therefore, *both* GRB and supernova Hubble diagrams are needed for a confident result.

4. IMPLICATIONS

Conceptually, the biggest question related to a construction of the GRB Hubble diagram is the possibility of luminosity evolution. Fortunately, there are two strong reasons that any such effects must be small. First, theoretical explanations for the luminosity indicators (Schaefer 2001; Ioka & Nakamura 2001; Plaga 2001) tie the relations to simple physics (involving relativistic effects operating on any light source, the delay in light traveling different paths, and the cooling of any body by radiation) that are unrelated to properties (such as metallicity) that might evolve. Second, just as for the purely empirical supernova Hubble diagram (Branch et al. 2001), any drift in population average properties (Lloyd-Ronning et al. 2002) is irrelevant, as the calibrations will work for any individual event whether near or far. That is, it does not matter whether population average properties (like luminosity) evolve, because the distances are derived for individual events that are each correctly calibrated.

Within 2 years, the GRB situation will be greatly improved with the dedicated *Swift* satellite (Gehrels 2000) currently scheduled for launch in 2003 September. *Swift* is expected to get ~100 bursts per year, of which ~40% will have directly measured redshifts. The redshift will be difficult to measure for $z > 6$ bursts, yet it is possible by locating the Lyman break with broadband photometry or spectroscopy extending into the near-infrared. In its nominal 3 yr lifetime, we can get ~120 bursts with measured values for z, P, $\tau_{\rm lag}$, V, and $E_{\rm peak}$. This many bursts will allow for high-accuracy calibration of the luminosity indicators. The large number of bursts will also allow for the reduction of statistical errors (dominated by the intrinsic scatter of the bursts) by a factor of ~10. If the bursts are divided into six redshift bins, each bin will have an error of 0.03 in the log of the distance. This accuracy will, for example, yield an uncertainty of ~0.03 in the derived value of Ω_m for a flat universe, even with no improvements in the luminosity indicators. So, with *Swift*, the prospect is that we can produce an accurate GRB Hubble diagram with ~120 bursts from $0.1 < z < 10$ by 2006.

What can we learn from the GRB Hubble diagram? We can test the predicted shift of the universe from matter to dark energy domination in the range $1 < z < 2$. We will also look for various predicted quintessence (Weller & Albrecht 1999) and nonstandard (Mannheim 2002) effects in the range $2 < z < 10$. The typical sizes of these effects are 0.4 in the log of the distance around a redshift of $z = 3$. The current paradigm of cosmology (the new inflation perhaps with quintessence) is so new and untested that surprises could easily await in the unknown regime of $z > 1$.

REFERENCES

Aguirre, A. 1999, ApJ, 525, 583
Brainard, J. J., Pendleton, G., Mallozzi, R., Briggs, M. S., & Preece, R. D. 1999, preprint (astro-ph/9904039)
Branch, D., Perlmutter, S., Baron, E., & Nugent, P. 2001, preprint (astro-ph/0109070)
Bromm, V., & Loeb, A. 2002, ApJ, 575, 111
Costa, E., et al. 1997, Nature, 387, 783
Durrer, R., & Novosyadlyj, B. 2001, MNRAS, 324, 560
Fenimore, E. E., & Ramirez-Ruiz, E. 2000, preprint (astro-ph/0004176)
Frail, D., et al. 1997, Nature, 389, 261
Gehrels, N. A. 2000, Proc. SPIE, 4140, 42
Hogg, D. W. 1999, preprint (astro-ph/9905116)
Ioka, K., & Nakamura, T. 2001, ApJ, 554, L163
Lamb, D. Q., & Reichart, D. E. 2000, ApJ, 536, 1
Lewis, G. F., & Ibata, R. A. 2001, MNRAS, 324, L25
Lloyd-Ronning, N., Fryer, C. L., & Ramirez-Ruiz, E. 2002, ApJ, 574, 554
Mallozzi, R. S., et al. 1995, ApJ, 454, 597
Mannheim, P. D. 2002, in AIP Conf. Proc. 624, Cosmology and Elementary Particle Physics, ed. B. N. Kursunoglu, S. L. Mintz, & A. Perlmutter (New York: AIP), 151
Moertsell, E., Gunnarsson, C., & Goobar, A. 2001, ApJ, 561, 106
Norris, J. P. 2002, ApJ, 579, 386
Norris, J. P., Marani, G. F., & Bonnell, J. T. 2000, ApJ, 534, 248
Paciesas, W. S., et al. 1999, ApJS, 122, 465
Perlmutter, S., et al. 1999, ApJ, 517, 565
Phillips, M. M., Lira, P., Suntzeff, N. B., Schommer, R. A., Hamuy, M., & Maza, J. 1999, AJ, 118, 1766
Plaga, R. 2001, A&A, 370, 351
Riess, A. G., et al. 2001, ApJ, 560, 49
Rossi, E., Lazzati, D., & Rees, M. J. 2002, MNRAS, 332, 945
Schaefer, B. E. 2001, preprint (astro-ph/0101462)
———. 2003, ApJ, 583, L71
Schaefer, B. E., Deng, M., & Band, D. L. 2001, ApJ, 563, L123
Totani, T., & Kobayashi, C. 1999, ApJ, 526, L65
van Paradijs, J., et al. 1997, Nature, 386, 686
Weller, J., & Albrecht, A. 2001, Phys. Rev. Lett., 86, 1939
Zhang, B., & Mészáros, P. 2002, ApJ, 571, 876